

AN OMNIDIRECTIONAL CONVECTION NULLING THERMOELECTRIC  
RADIOMETER FOR ENVIRONMENTAL APPLICATIONS

by

DAVID LLOYD BRAUN

B. S., South Dakota School of Mines, 1961

---

A MASTER'S THESIS

submitted in partial fulfillment of the

requirements for the degree

MASTER OF SCIENCE

Department of Mechanical Engineering

KANSAS STATE UNIVERSITY  
Manhattan, Kansas

1967

Approved by:

  
Major Professor

LD  
2668  
T4  
1967  
B675

## TABLE OF CONTENTS

Chapter	Page
I. INTRODUCTION. . . . .	1
II. REVIEW OF THE LITERATURE. . . . .	3
Summary of Existing Instruments. . . . .	3
Comparison of Existing and Proposed Instruments. . . . .	5
III. THE RADIOMETER DESIGN . . . . .	7
Design Alternates. . . . .	7
The Radiometer Design and Construction . . . . .	10
IV. THEORETICAL DISCUSSION. . . . .	19
The Sensing Element Energy Balance . . . . .	19
Error Signal Generation. . . . .	26
Transient Response . . . . .	27
V. THE CONTROLLER DESIGN . . . . .	29
Basic Control Objectives . . . . .	29
The Power Supply Design. . . . .	30
Automatic Control of Thermoelectric Current. . . . .	32
Optimization of Control Functions. . . . .	37
VI. THE RESULTS . . . . .	41
LIST OF REFERENCES . . . . .	47
APPENDIX . . . . .	49

LIST OF TABLES

Table	Page
1. Results of Test Chamber MRT Measurements . . . . .	.43
2. Temperature Gradient Calculations for the Sensing Element . . . . .	.51
3. Radial Heat Transfer Calculations for the Heat Meter Insulation. . . . .	.54
4. Error Signal Calculations . . . . .	.63

## LIST OF FIGURES

Figure	Page
1. Alternate Sensing Element Designs . . . . .	8
2. The Radiometer Design . . . . .	.13
3. The Heatsink Design . . . . .	.15
4. Photograph of Radiometer and Heatsink Components. . . . .	.18
5. Energy Balance for Sensing Element at Ambient Air Temperature. . . . .	.19
6. Use of Black, Grey, and Pink Coatings for MRT Measurements . . . . .	.22
7. Spectral Reflectance Curve for Radiometer and Human Skin . . . . .	.25
8. Theoretical Deviation of Sensing Element Temperature from Still Air Temperature of 70F. . . . .	.25
9. Transient Heating and Cooling Curves of the Spherical Sensing Element. . . . .	.28
10. The Power Supply Schematic. . . . .	.31
11. Photograph of Controller Mechanism. . . . .	.34
12. The Controller Schematic. . . . .	.38
13. Controller Performance at Different Sensitivity Settings . . . . .	.40
14. Photograph of Complete Radiometer Systems . . . . .	.42
15. Model for Sphere Temperature Gradient Calculations. . . . .	.50
16. Model for Heat Meter Error Calculations . . . . .	.53

## CHAPTER I

### INTRODUCTION

The current standard for describing an environment from a radiation heat transfer standpoint is the Mean Radiant Temperature (MRT). The Mean Radiant Temperature is the temperature of a uniform black enclosure in which a solid body or occupant would exchange the same amount of radiant heat as in the existing non-uniform environment (2). In an environment where surface temperature varies from point to point the MRT will vary with all three coordinates in space.

MRT is an important variable in human comfort studies as well as in other heat transfer analyses. Herein the primary emphasis is placed upon the MRT in relation to the thermal exchanges of the human body and his environment.

Measurement of MRT is difficult because the effects of radiation must be separated from other heat transfer effects. Considerable effort has been directed towards the development of the several existing instruments capable of measuring MRT. All of the instruments account for convection and conduction effects by some means. None of them, however, completely eliminate convection effects over the range of MRT above and below the ambient air temperature. For an exposed sensing element this implies that surfaces which absorb or emit radiant energy must be

controlled at a temperature equal to the average of the surrounding air temperatures.

As originally outlined, the object of the research described herein was to develop an instrument using thermoelectric heating or cooling which could be used to measure the MRT with respect to the human subject, and which accounted for convection effects by nulling them. This thesis describes the design, construction, and operation of such an instrument.

The basic idea of using a thermoelectric module for this purpose was first made known to Dr. Preston E. McNall by Robert H. Tull of the Electric Space Conditioning Institute in Morristown, New Jersey.

## CHAPTER II

### REVIEW OF THE LITERATURE

#### Summary of Existing Instruments

A literature survey was made to determine the state of the art for thermal radiometers. The period considered in the survey was from about 1950 to the present. Developments prior to 1950 were not considered for reasons soon to be made apparent.

A two-sphere radiometer was developed by Minneapolis Honeywell in the early 1950's. The early phases of this project included an extensive survey of applicable radiometers in use at or before that time. The Honeywell research report constitutes a major reference for this author (17). The operating principle of this radiometer is that if two geometrically identical spheres are controlled at the same preset temperature, somewhat above ambient air temperature, conduction and convection losses are equal for the two spheres. If one sphere is black and has a high emissivity and the other is polished gold and has a low emissivity the radiation losses are different. Therefore, the difference in power inputs required to keep the spheres at equal temperatures depends upon radiation effects alone. This difference in power inputs to the two spheres is related to the MRT. The reported accuracy of this instrument is  $\pm 2F$ .

Aagard (1) developed the only truly convection-free instrument included in the survey. Aagard's radiometer is composed of a spherical element of known emissivity which is electrically heated to replace radiation losses. The amount of electrical heating is just sufficient to keep the sphere at the ambient air temperature. This instrument is used only when the MRT is below air temperature. The primary application is the determination of radiation losses to the night sky.

Other instruments which integrate radiation effects over a  $4\pi$  enclosure have been developed by Richards, Stoll, and Hardy (15) and by Benzinger and Kitzinger (4). The former instrument is similar in some respects to the Honeywell two-sphere radiometer. Four geometrically identical spheres are each internally heated. One sphere is black, one white, and the remaining two are highly polished. Total environmental thermal radiation is obtained by measuring the heat input to the two spheres of lower temperature to bring the black, white, and one polished sphere to the same temperature. The second polished sphere is used to provide for wind velocity measurements. MRT readings may be made with an accuracy of  $\pm 1.8\text{C}$ , or about  $\pm 3.2\text{F}$ .

The instrument of Benzinger and Kitzinger consists of foil surface receivers which can be arranged in a variety of shapes. The receivers are thermoelectric generators and are used to line a cavity surrounding a source of radiation. Actually instruments heretofore discussed measure effective surface temperatures from a point in space allowing us to calculate the radiant losses

from a body. This instrument directly measures those radiation losses over a  $4\pi$  solid angle by surrounding the radiating body. Response time is 2.4 seconds, notably faster than other radiometers studied.

Less noteworthy for this study are several radiometers for meteorological work. Houghton and Brewer (12) describe an instrument which integrates effects over a  $2\pi$  solid angle. A high vacuum in conjunction with an infra-red transmitting window minimizes effects of convection heat exchange. In an instrument designed by Funk (7), polythene windows are heated to prevent dew formation which has the effect of "blackening" the polythene surface.

Instruments by Tunmore (19), Moran (14), Treharne and Trolander (18), Hager (11), and Stoll (16) are all directional in nature. Of these, Stoll's instrument is applied to environmental studies. It has been used for skin temperature measurements in ambient temperatures ranging from normal room temperature to  $-45^{\circ}\text{C}$ .

#### Comparison of Existing and Proposed Instruments

Of the instruments studied, Aagard's convection-free radiometer most closely relates to the proposed instrument. In both, the sensing element surface is controlled at ambient air temperature. The Aagard radiometer, however, has no refrigeration capability and hence may be used only when the MRT is lower than air

temperature. The proposed instrument will be compatible with environments in which the MRT is both higher and lower than air temperature.

The Minneapolis Honeywell and the Hardy radiometers are both used to measure the MRT when it is above or below air temperature. Therefore, any improvements to be made fall into the area of accuracy and convenience. The Minneapolis Honeywell radiometer is considerably more accurate than the Hardy radiometer. The proposed instrument is expected to further increase the accuracy of MRT readings. It is also to be completely automatic such that it may be operated for long periods with no operator present.

The other articles referred to were helpful in a more general way. They have provided much of the necessary background for the study which follows.

## CHAPTER III

### THE RADIOMETER DESIGN

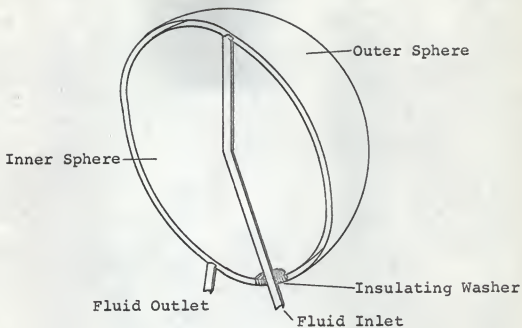
#### Design Alternates

There are many possible ways of maintaining a surface at a constant temperature while removing heat from it or supplying heat to it. All possibilities must involve heat transfer of some kind. This heat transfer may be accomplished using a mass transfer phenomenon or by heat transfer alone.

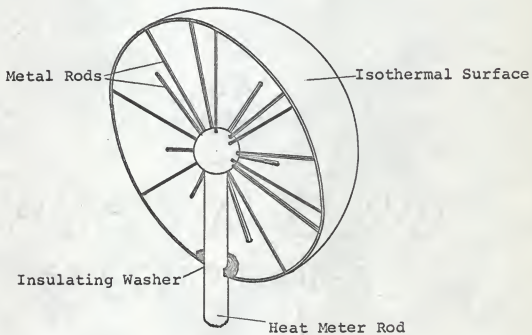
The first approach to the problem employed a mass transfer device. In Fig. 1a is shown the sensing element design. Fluid flows continually through the space between the two spheres and is used to remove energy from or to supply energy to the surface of the outer sphere. In so doing the fluid changes temperature. Knowledge of this temperature change and the fluid flow rate is sufficient for an energy balance.

Control is accomplished by sensing the average of inlet and outlet temperatures and controlling this average equal to the ambient air temperature. Two constant temperature reservoirs and a mixing valve provide the inlet fluid at the desired temperature level.

This method is attractive from the standpoint of a possible fast response time. Difficulties are the control of flow rate



(a) Mass Transfer



(b) Conduction Heat Transfer

Figure 1. Alternate Sensing Element Designs

and fluid temperatures. A preliminary calculation was made to determine the feasibility of using this method with water as a working fluid. Conditions were set so that the water would remove 10 Btu/hr from a two inch "blackened" spherical sensing element. This corresponds to MRT conditions of 140F with an ambient air temperature of 40F. The product of mass flow rate (lbs/hr) and temperature rise (F) is 10. Therefore, even for this extreme measurement, the flow rate would have to be low or the temperature rise slight or both. Based on these conclusions, difficulties in control, and difficulty of construction, no further study was expended towards a mass transfer solution.

All other alternatives considered were of the type using heat conduction in a metal rod. This provides for transport of thermal energy to or from the sensing element. It also provides for measurement of the magnitude of this energy. Figure 1b shows one idea for satisfying the constant surface temperature criterion. Here each heat flow path is of the same geometrical configuration so that the ends of all the small rods form an approximately isothermal network. Expected difficulty in building such a device induced a careful look at the proposal described below.

Suppose that heat were transferred to or from the sensing element through a rod connected to the skin of the sensing element at only one small area. This means that the skin of the element would have to convey heat to the transfer area. This immediately implies surface temperature gradients and appears to

violate a basic design criterion. The problem of calculating these gradients is treated in the error analysis, Appendix A. The results indicate that for measuring an MRT of 130F in ambient air at 70F the maximum difference in temperature between the top of a two inch hollow silver sphere 0.020" thick is less than 0.5F. This represents an acceptable error to this author. Additionally, this method is the most simple of the previous alternatives and has become the basis for the present design.

#### The Radiometer Design and Construction

There are several factors to be considered in selection of a material for the radiometer. Thermal conductivity should be high to minimize the gradients on the sensing element skin. The thermal diffusivity, or the quotient of conductivity divided by the product of density times specific heat, should be high so that response time is kept at an acceptable minimum. A reasonable mechanical strength is desired even though the instrument is to be considered delicate.

A check of common metals revealed that silver is 10 percent above copper in thermal conductivity. This advantage does not offset the considerably higher cost of silver. Silver is, however, 50 percent better than copper in terms of thermal diffusivity. In addition to this advantage, silver is easily cold-worked, and has sufficient strength. The cost is not prohibitive for the small amounts being considered. Based on these considerations, silver was used.

A necessary limitation of this study and an area where future emphasis may be placed is the consideration of shape factor for the sensing element. The instrument is to be insofar as possible a human analog. It should therefore approximate a human figure in terms of shape factor. Primary emphasis in this study is directed towards development of the radiometer and the radiometer control principles.

A spherical shape was chosen for the sensing element. This is the only shape which measures an entirely non-directional MRT (15). For human comfort work there are many geometrical attitudes which may be assumed by the body in exchanging radiant energy with his surroundings. The spherical shape will approximate a large portion of these attitudes.

Sizing of the spherical element is dependent upon several considerations. The surface area must be sufficient to receive or emit a measurable amount of radiation energy. The sphere must be large enough so that the thermoelectric module and its heat sink subtend only a small solid angle. The thickness of the sphere wall must be great enough to provide for a degree of mechanical strength and also to keep sphere temperature gradients at a minimum. Lastly, the amount of metal must be kept as low as practicable for fast time response. After weighing each of the above factors a sphere of two inch diameter and 0.020" wall thickness was decided upon.

Several attempts to purchase hollow silver spheres were unsuccessful. Metal spinning provides an easy solution to the

problem but a chance conversation<sup>1</sup> revealed a unique method (see Appendix B) for forming the spheres without using the spinning process. Figure 2 shows the sphere in relation to other radiometer components.

The difference in temperature between the sphere and the ambient air is sensed by a differential thermopile. The thermopile used for the sphere temperature is composed of 4 couples as is the one measuring the air temperature. The air temperature sensor is shielded to minimize radiation effects and to obtain a true reading of the air temperature.

The heat meter rod was sized by practical and experimental considerations. Factors were 1) the mass of the rod should be kept at a minimum, 2) the length of the rod should be sufficient to allow the thermoelectric equipment to subtend a small solid angle, and 3) temperature gradients in the rod should be measurable for the smallest reading desired and not excessive for the largest reading to be made. Rods of copper were experimented with in the first radiometers built for this study. The ideal size has been found to be about 5 to 6 inches in length and about 3/16 inches in diameter.

The analysis of the heat meter circuit is given in Appendix C. The number of thermocouples used and their spacing is predetermined so that the millivolt output of the heat meter is numerically equal to the heat conducted in Btu/hr. Thus for a

---

<sup>1</sup>Mr. Robert Tagliatela, machinist with Continental Oil Co., Ponca City, Oklahoma is credited with the described method.

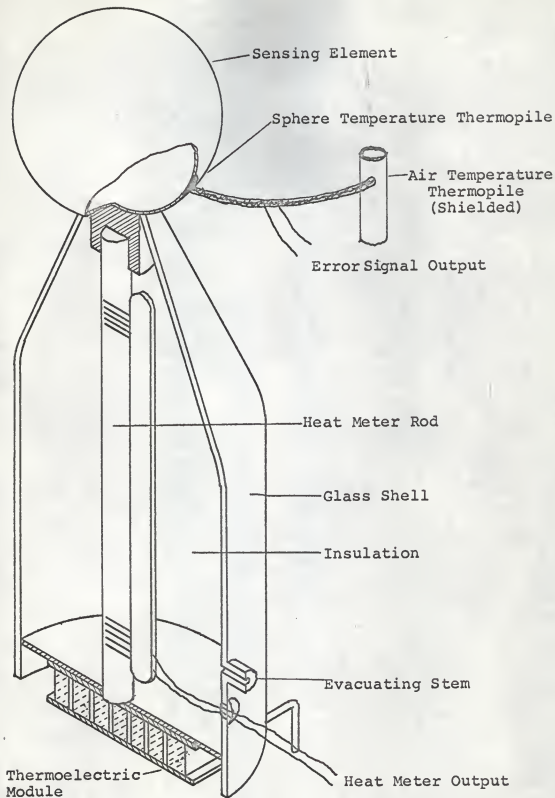


Figure 2. The Radiometer Design

one millivolt reading, one Btu/hr flows in the metering rod. The slight nonlinearity of thermocouple response curves causes a small error as discussed in Appendix C.

A glass shell filled with a micro-cell powder insulation and later evacuated, is used to reduce radial heat flow to or from the metering rod to a very low level. The powder is Santocel A made by Monsanto Chemical Company. On page 117 of his book, Bell discusses use of this powder in cryogenic applications (3). A calculation of radial heat flow is included in Appendix A and shows that this component is below 1/2 percent of the axial component.

The thermoelectric module is coupled to the metering rod by means of a thin plate. This plate is sealed to the glass shell with epoxy cement. A thin layer of a silicon type, heat conducting grease is placed between the thermoelectric module and the coupling plate.

Sizing of the thermoelectric module was accomplished by reference to manufacturers specifications. It was necessary to increase the module size during the developmental phase to provide for efficient module operation at low current levels. The present 32 couple module was purchased from Frigistors Ltd., a Canadian firm.

The heat sink system is shown in Fig. 3. The radiometer is bolted to the heat sink proper with pressed wood studs. These prevent a high conductivity thermal short circuit across the thermoelectric module. The design of the heat sink provides for positive air circulation with a minimum mixing of inlet and

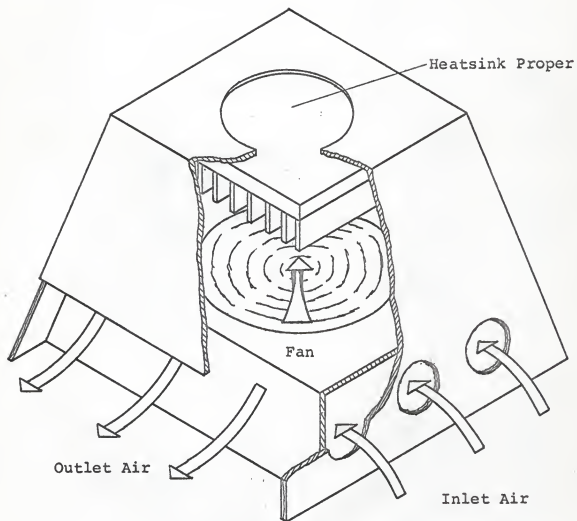


Figure 3. The Heatsink Design

outlet air. Air enters below the fan by way of the circular holes. Next, the fan forces the air into the fins of the heat sink proper. The air then flows out at 90° to the entrance angle and is deflected downward. This minimizes currents around the sensing element which is located 6 inches above the top of the heat sink. For low thermoelectric currents (below 1 amp) natural convection is sufficient for cooling of the heat sink fins, and the fan is not needed. These low current levels are associated with an MRT only slightly above or below the ambient air temperature. For these readings errors due to air currents around the sensing element become more critical. Therefore, a control feature is added to automatically energize the fan at currents of 1 amp or more, and to shut off the fan at currents below 1 amp.

Smoke tests of the heat sink indicate that in a still room there is only a slight secondary effect by which air from above the sphere is pulled downward by the outlet sink air.

At maximum thermoelectric current (5 amps) the temperature rise of the air through the heat sink is less than 2F. The heat sink surfaces operate at a temperature of about 3F higher than the ambient air temperature for this maximum case. The radiometer will operate at current levels not to exceed 5 amps. At this level of current, the module is capable of removing about 7 Btu/hr from the sensing element. This means that a MRT of about 130F may be measured in an ambient temperature of 70F. These figures are included to show that the slight temperature rise of the heat sink will not introduce errors of any consequence.

The completed instrument proper is shown in Fig. 4. The connections from the base of the heat sink are for the DC signal to the thermoelectric module (Amphenol Plug), the AC power for the fan (recessed plug), and the thermocouple circuits (opposite side).



Figure 4. Photograph of Radiometer and Heatsink Components

## CHAPTER IV

### THEORETICAL DISCUSSION

#### The Sensing Element Energy Balance

The sensing element heat balance equation for a given interval of time is

$$Q_i = Q_o + \Delta E \quad , \quad [1]$$

where  $Q_i$  = Net energy influx by radiation, conduction, and convection (Btu),

$Q_o$  = Net energy outflux by radiation, conduction, and convection (Btu),

$\Delta E$  = Changes in the sensing element stored energy (Btu).

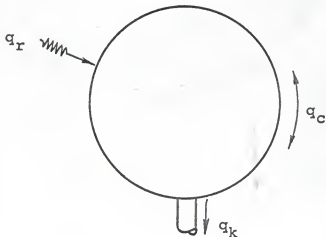


Figure 5. Energy Balance for Sensing Element at Ambient Air Temperature

With reference to Fig. 5, when the instrument is operating with the sensing element temperature constant and equal to the

ambient air temperature [1] may be reduced to

$$q_r = -q_k \quad , \quad [2]$$

since

$$q_c = 0 \quad . \quad [3]$$

In these equations,

$q_r$  = Net radiant energy influx or outflux (Btu/Hr) ,

$q_k$  = Net conduction energy influx or outflux  
(Btu/hr) ,

$q_c$  = Net convection energy influx or outflux  
(Btu/hr) .

For a steady state condition [2] may be expressed as

$$K_r A_r \frac{\Delta T_r}{\Delta X_r} = \sigma F_e F_a A (T_S^4 - T_{MRT}^4) \quad , \quad [4]$$

where

$K_r$  = Thermal conductivity of heat metering rod, (Btu/hr F ft) ,

$A_r$  = Cross sectional area metering rod (ft<sup>2</sup>)

$\Delta T_r / \Delta X_r$  = Temperature gradient on heat metering rod (F/ft) ,

$\sigma$  = Stefan Boltzmann constant (5) , (Btu/hr ft<sup>2</sup>R<sup>4</sup>) ,

$F_a$  = Angularity factor; unity for small objects in large enclosures (5) , (Dimensionless) ,

$F_e$  = Emissivity factor; for small objects in large enclosures equal to the emissivity of the small object (5) , (Dimensionless) ,

$A$  = Sensing element surface area ( $\text{ft}^2$ ),

$T_S$  = Sensing element surface temperature (R),

$T_{\text{MRT}}$  = Mean Radiant Temperature of the surrounding surfaces (R).

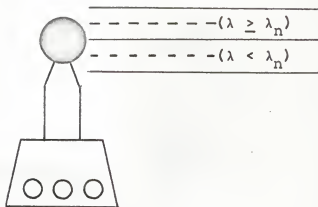
For  $T_{\text{MRT}} > T_A$  as is the case in Fig. 6, the right and left sides of [4] are negative. For  $T_{\text{MRT}} < T_A$  both sides are positive. This results in a thermodynamically correct situation considering the sphere as the system and the metering rod as a heat source or sink.

All of the foregoing may be readily applied in cases where  $F_e$  is a constant value for all wavelengths (greybody). The use of such a coating satisfies all requirements for measurement of MRT. In the definition of MRT no mention is made of the emissivity of the body exchanging radiation with the enclosure. The idea in determining MRT is to replace the given variable temperature enclosure with a uniform "black" enclosure such that there is no change in the total heat exchanged by the body and the enclosure.

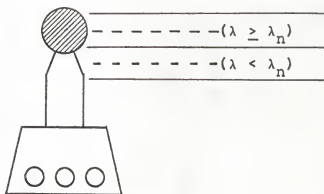
Is there then a unique MRT value for an object of given shape and temperature in a given enclosure with a given temperature distribution? The answer may be found by referring to Fig. 6 and the following illustration.

Consider three instruments identical in all respects except surface emissivity. Instrument A has an emissivity of unity for all wavelengths. Instrument B has an emissivity of 0.5 for all wavelengths. Instrument C has an emissivity of unity for all

Instrument A  
 $F_e = 1.0$   
 (black)



Instrument B  
 $F_e = 0.5$   
 (grey)



Instrument C  
 $F_e = 1.0(\lambda \geq \lambda_n)$   
 $F_e = 0.5(\lambda < \lambda_n)$   
 (pink)

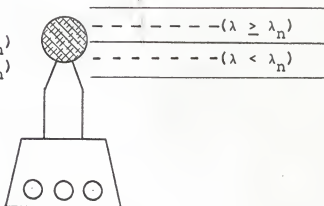


Figure 6. Use of Black, Grey, and Pink Coatings for MRT Measurements

wavelengths above or equal to  $\lambda_n$  and an emissivity of 0.5 for all wavelengths below  $\lambda_n$ . All three instruments are used to find the MRT in an enclosure ( $T_{MRT} > T_A$ ) radiating energy in two equal parts above and below  $\lambda_n$  in wavelength.

Using [4], instrument B receives one-half the energy received by A, but this is exactly accounted for by adjustment of the value of  $F_e$ . Therefore, both A and B read the same value for the MRT. Instrument C receives three-fourths of the energy received by A. To interpret this heat flow suppose that all three instruments read the same value of MRT. This implies that the value of  $F_e$  for C is 0.75. Then the original environment may be replaced by a uniform "black" enclosure at  $T_{MRT}$ . It is clear that the heat flow to instruments A and B would remain the same. The heat flow to instrument C would increase because all of the incoming radiation would now be of wavelength greater than  $\lambda_n$ . Since the heat flow to C increased, the value of MRT it was "measuring" is incorrect. Therefore the value of  $F_e$  for C is not 0.75.

Now suppose  $F_e$  for instrument C is taken as unity. Then the value of MRT it would read would be below the MRT as read by A and B. Replacing the original enclosure with a black enclosure uniformly at this lower value of MRT would not change the net heat flow because the incoming radiant energy is all above  $\lambda_n$  in wavelength. Thus using unity for the  $F_e$  of C results in a "correct" reading of MRT but one which is lower in magnitude than the MRT read by A and B. This means that MRT is dependent upon

the degree of departure from surface "greyness" or from uniformity of spectral emissivity of the body measuring MRT.

The importance of these considerations is in the fact that the human skin has a variable reflectivity. Figure 7 illustrates this fact. It has been noted by Gagge (8) and others that instruments with a constant  $F_e$  tend to give higher estimates of MRT than are given by human subjects. This effect is most pronounced when there are large amounts of energy in the visible spectrum.

It is now clear that use of a surface coating with a spectral reflectivity curve approximating that of the human skin will result in readings of MRT which are more realistic for human environmental studies. Further, it has been pointed out that use of an  $F_e$  equal to the absorptivity of the surface coating at longer wavelengths results in correct computation of MRT. The paint whose spectral reflectivity is shown in Fig. 7 is used on the present instrument. From this the value for  $F_e$  is taken as 0.87 at the long wavelengths.

Using this value and the other known parameters in consistent units (see Appendix C) [4] becomes

$$K_r A_r \frac{\Delta T_r}{\Delta X_r} = 0.012023 \left[ \left( \frac{T_S}{100} \right)^4 - \left( \frac{T_{MRT}}{100} \right)^4 \right] \quad [5]$$

Both sides of [5] are in units of Btu/hr. This equation is used to calculate values of MRT when the sphere temperature  $T_S$  equals the ambient air temperature  $T_A$  and when the heat meter reading and either  $T_S$  or  $T_A$  are known. The equation has been

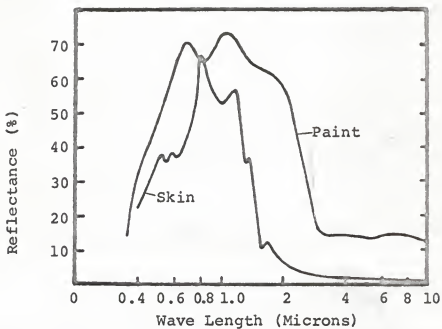


Figure 7. Spectral Reflectance Curve for Radiometer Coating and Human Skin (Courtesy Minneapolis Honeywell)

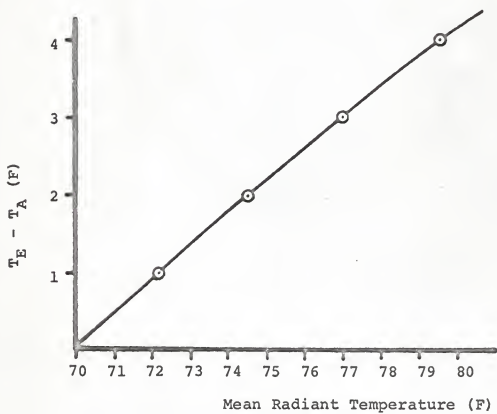


Figure 8. Theoretical Deviation of Sensing Element Temperature from Still Air Temperature of 70F.

solved for  $T_A$  and  $T_{MRT}$  ranging from 510 to 580 R in increments of one degree. A tabulation of heat readings versus  $T_A$  and  $T_{MRT}$  is available to users of the instrument.

Another environmental parameter, the Effective Radiant Field (ERF), (8) is directly measured with this instrument. The Effective Radiant Field is defined as the radiant heat which would be exchanged by a room occupant with the surrounding surfaces if his skin or clothing were hypothetically equal to the ambient air temperature. The magnitude of  $q_k$  or  $q_r$  is directly related to the ERF.

#### Error Signal Generation

When the sensing element is first placed in position for a measurement the temperature of the sensing element will approach a value ( $T_E$ ) somewhere between  $T_A$  and  $T_{MRT}$ . The error signal to be used for the controller operation will depend on the difference of  $T_E$  and  $T_A$ . To aid in the controller design, the following estimates of this difference are made.

Assume that the base of the heat metering rod is at  $T_A$ , and that the top of this rod is at  $T_E$ . After steady state conditions are reached the sensing element experiences all three modes of heat transfer. For  $T_{MRT} > T_A$  the following is true,

$$q_r = q_c + q_k \quad [6]$$

Substitution of known and assumed parameters (see Appendix D) results in

$$0.012023 \left[ \left( \frac{T_{MRT}}{100} \right)^4 - \left( \frac{T_E}{100} \right)^4 \right] = 0.0501 (T_E - T_A)^{1.25} + 0.103 (T_E - T_A) \quad . \quad [7]$$

The solution of this equation is approached by assuming a value for  $T_A$ , and a set of values for  $T_E$ .  $T_{MRT}$  is solved for.  $T_A$  is assumed to be 70F.  $T_E$  is varied from 70F to 80F in one degree increments. The results are plotted in Fig. 8 and give an indication of the error signal to be expected for a given MRT.

#### Transient Response

One criterion for controller design is that the sphere temperature be controlled. Therefore, the design of the controller will depend upon the speed with which the sphere temperature can be changed. A change in sphere temperature occurs with a change in the current flowing to the thermoelectric module.

The temperature response of the sphere to a step change in thermoelectric module current was experimentally determined. Curves were generated for both sphere heating and cooling. The results (Fig. 9) give a clear indication of the time interval between successive adjustments of thermoelectric module current.

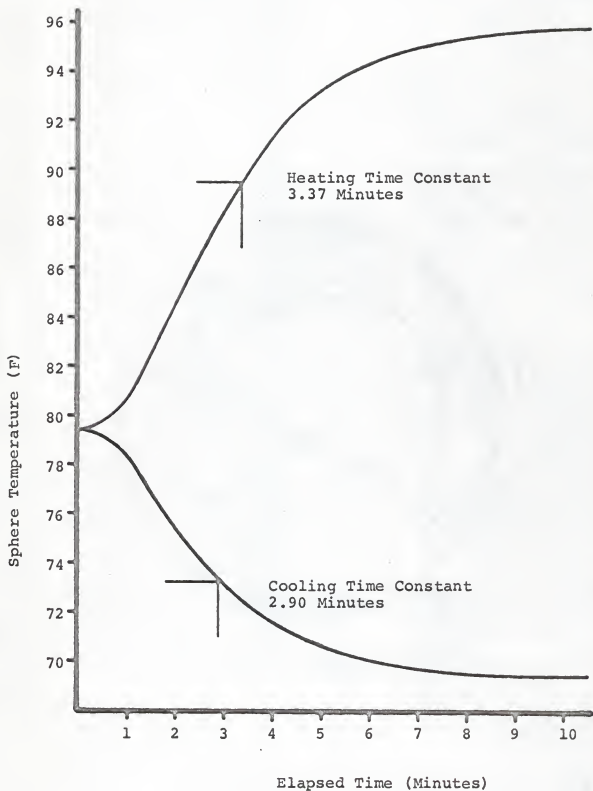


Figure 9. Transient Heating and Cooling Curves of the Spherical Sensing Element

## CHAPTER V

### THE CONTROLLER DESIGN

#### Basic Control Objectives

In Chapter IV the concept of initial error signal was introduced. In essence the controller must sense this initial error signal and cause it to go to zero. Further, the controller must continually monitor the error signal and retain it at or near the zero value. This results in the average sphere temperature being held equal to the average ambient air temperature.

Several other control functions are added. The first of these is a means of reading the error signal. This allows the operator of the instrument to visualize the actual error, make adjustments for overshooting, and note rapid changes in thermal conditions. Secondly, an estimate of the heat flowing in the metering rod may be made. For precision measurements the radiometer must be used in conjunction with an accurate potentiometer or recorder. A third control function insures that no readings are taken during conditions of transient heat flow. Thus the instrument controller will indicate when steady state conditions exist in the metering rod. Finally, the heat sink fan operation is to be controlled.

The possibilities for synthesis of a controller to perform these tasks are numerous. Considering availability of material

and economic factors, one solution is dominant. This centers on the use of the continuous balance principle by which small DC voltages may be translated into proportional mechanical deflections. The small voltages are derived from the error signal. The mechanical deflections are used to control the output of the power supply described next.

### The Power Supply Design

The use of a thermoelectric module prescribes that the primary output of the controller must be a DC current signal. The magnitude and sign of this current flow with respect to the module determines the amount and direction of heat flow in the metering rod. Because heat flow is to be both positive and negative with respect to the sensing element, the power supply must be capable of a polarity reversal. Further considerations will require that a smooth reversal of polarity be accomplished with a rotation of a single shaft. This is easily done with a center-tap potentiometer but this is a highly dissipative method because the largest value of current to be used must continually flow in the potentiometer coil. After considerable experimentation with several other dissipative methods a non-dissipative solution was found.

Figure 10 is a schematic of the power supply. There are separate circuits for sphere heating and sphere cooling. The choke coil and ammeter are common to both circuits.

The breakover micro-switch, M5 controls the polarity at the output terminals. A clockwise rotation of the cam upon which this

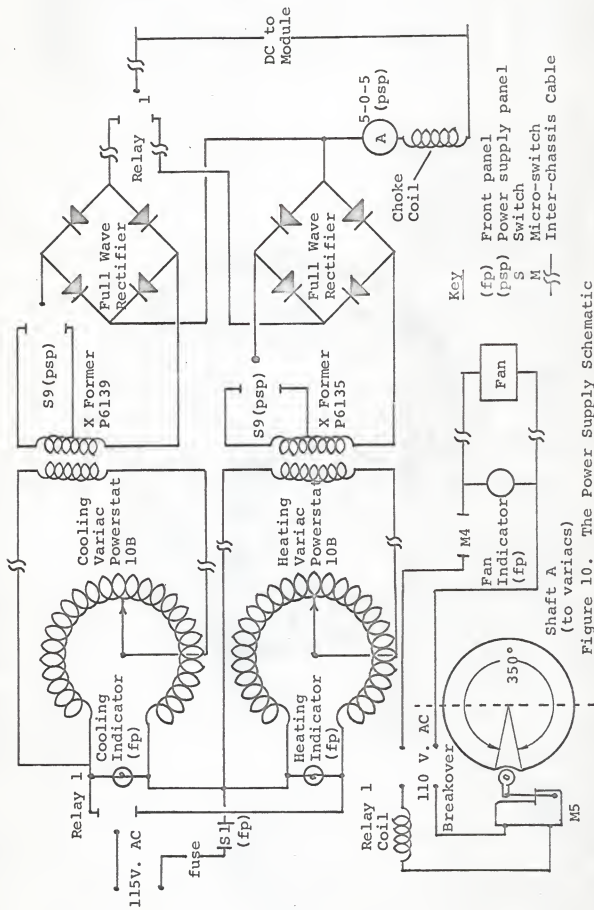


Figure 10. The Power Supply Schematic

switch rests breaks the circuit through M5. This relaxes the relay coil R1 resulting in a closing of the cooling variac contacts and in a closing of the DC portion of the cooling power supply. A counter clockwise rotation of the switching cam makes a circuit through M5 and engages R1. This energizes the heating variac and also the DC portion of the heating power supply. Note that a counter clockwise cam rotation results in a "breakover" action of M5 for 350° of cam rotation. From the position shown the power supply shaft may be turned 350° in either direction for smooth increases of either heating or cooling.

The fan control cam operating M4 insures that the heat sink fan is off when thermoelectric current is below 1 amp. When the current exceeds this value the fan is automatically turned on.

The center tap of both the heating and cooling transformers may be used by switching S9. This lowers the thermoelectric current level at a given variac shaft setting. This will allow added flexibility for controller optimization.

#### Automatic Control of Thermoelectric Current

The present control system may be classified as a sample-data system. According to a definition by Gibson (9) a sample data system is a control system in which information is transmitted only at discreet intervals called sampling intervals rather than continuously as in conventional systems. The time period between sampling intervals is related to the previously determined time response of the complete radiometer system.

In order to properly explain the controller operation some groundwork is needed. The continuous balance principle can provide a method for deflecting the power supply shaft based on the magnitude and polarity of the DC error signal. Suppose that the power supply were directly coupled to the balance unit (proportional control). An error signal would then deflect the balance unit and the power supply shaft resulting in a flow of current to the thermoelectric module. This current would then begin to reduce the error signal which would in turn reduce the amount of current. It is clear that this method cannot possibly result in a zeroing of the error signal. From this it is concluded that no permanent connection between the power supply and the balance unit may be made. This implies the use of a clutching mechanism.

Figure 11 is a plan view photograph of the controller components. The magnetic clutch, labeled 9, allows the power supply variacs, 7 and 8, to be coupled and uncoupled from the servo motor, 6, balance potentiometer, 4, and amplifier, 1.

The heart of the control mechanism is the cycle timer, 10. Three cams rotate together. The outside cam, operating M3, is used to engage or disengage the magnetic clutch. The middle cam, operating M2, determines whether the error signal or the heat meter signal will be sampled. The inner cam, operating M1, determines whether or not any signal will be sampled. The raised portion of this cam corresponds to a short circuit so that zero voltage is read.

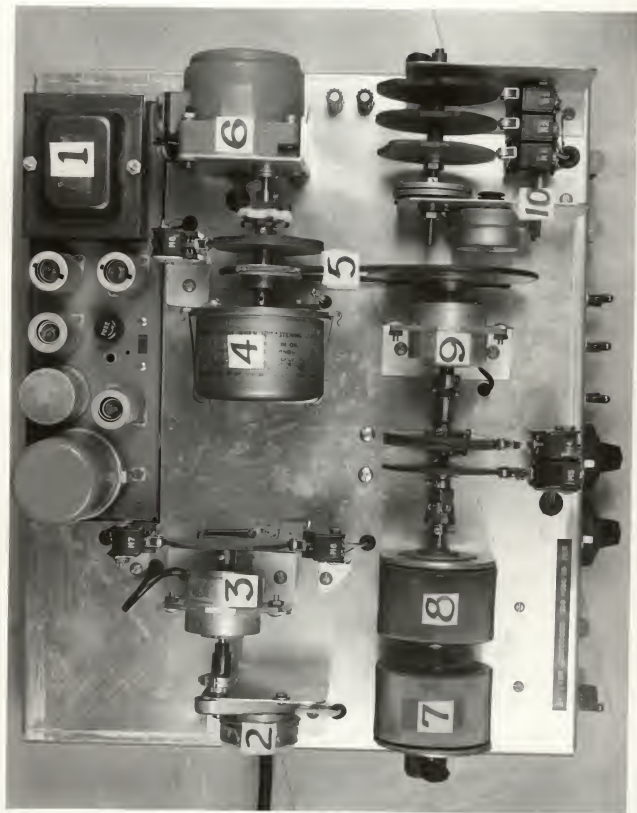


Figure 11. Photograph of Controller Mechanism

As the cycle timer rotates the sequence of events is as follows:

1. Read zero voltage
2. Read heat meter gradient voltage
3. Read zero voltage
4. Engage magnetic clutch
5. Read error signal voltage
6. Disengage magnetic clutch
7. Read zero voltage

These steps constitute a complete cycle of control operation. Steps 2 and 5 are steps during which sampling actually takes place. Note that when the error signal is read, the clutch is engaged. This causes a deflection of the balance unit servo shaft which is transmitted thru the belt, 5, to the input clutch shaft, and on to the variac units. Then the clutch is disengaged while the variac shaft is in the displaced position. Following this, the balance unit returns to zero deflection (step 7). By these means the variac shaft is left in the displaced position. The angular rotation of the variac shaft is proportional to the magnitude and sign of the error signal. Thus when the error signal is large, a large adjustment is made to the thermoelectric current. If the error signal is zero, no adjustment is made because the sphere surface temperature and ambient air temperature are equal.

The time period for one cycle is set equal to the longer of the time constants found in Fig. 9. This results in a cycle time of 3-2/3 minutes.

Recall that one of the control objectives was to insure that heat meter readings are made only when the radiometer systems are at steady state. With each movement of the servo-motor shaft there is a transient condition set up in the radiometer. Therefore the motion of the servo-motor shaft must be monitored. The transient timer mechanism is used for this purpose. As seen in Fig. 11 and Fig. 12, it is composed of the switch, M8, the magnetic clutch, 3, the 1/20 rpm motor, 2, and switches, M6 and M7. When the balance shaft is at the zero position M8 is closed and current flows to the magnetic clutch, 3, locking it. This allows the motor, 2, to turn the cam controlling M6 and M7. If the balance shaft does not move for a period of 4 minutes the motor, 2, will have advanced the cam upon which M6 and M7 rest to a point where M6 changes position, turning the red pilot (transient indicator) off and turning the white pilot (steady state indicator) on. About 10 seconds later M7 turns the motor, 2, off. This prevents further motion of the cam. When the balance shaft moves, indicating a difference in temperature of the sphere and its surrounding air, the current to the magnetic clutch, 3, is interrupted. This releases the clutch and resets M6 and M7. M6 returns to the transient position and M7 is closed turning the timer, 2, on.

The net effect of the transient timer mechanism is to control the transient and steady state pilot lights. If there are two successive sampling periods with no motion of the balance shaft the temperatures of the sphere and surrounding air are equal and no further adjustment of thermoelectric current is required. The steady state pilot light (white) will then be

energized. Should external conditions change, the sphere temperature will change and the balance shaft will deflect, resetting the transient timer. This will energize the transient pilot light (red) indicating a change in thermoelectric cooling or heating load with a corresponding transient in the heat metering rod. This indicates that no reading should be made.

Figure 12 is the controller schematic. Many of the components have previously been discussed. The sensitivity adjustment R1 changes the voltage drop across R2 which changes the angular deflection of the balance shaft given a constant input signal.

The DPDT switch, S-8, provides for internal or external readout of the heat meter signal. When using external readout, S6 is placed in the closed position.

S2, S3, and S4 are each used for energizing various controller components.

#### Optimization of Control Functions

In the radiometer design a fair amount of emphasis was placed upon providing for a fast response time. It is therefore logical and necessary to make use of this design foresight by optimization of the controller. The length of time necessary for the error signal to go to zero is to be made as short as possible. This study also provides knowledge of the sensitivity settings which result in underdamped, critically damped, and overdamped temperature response.

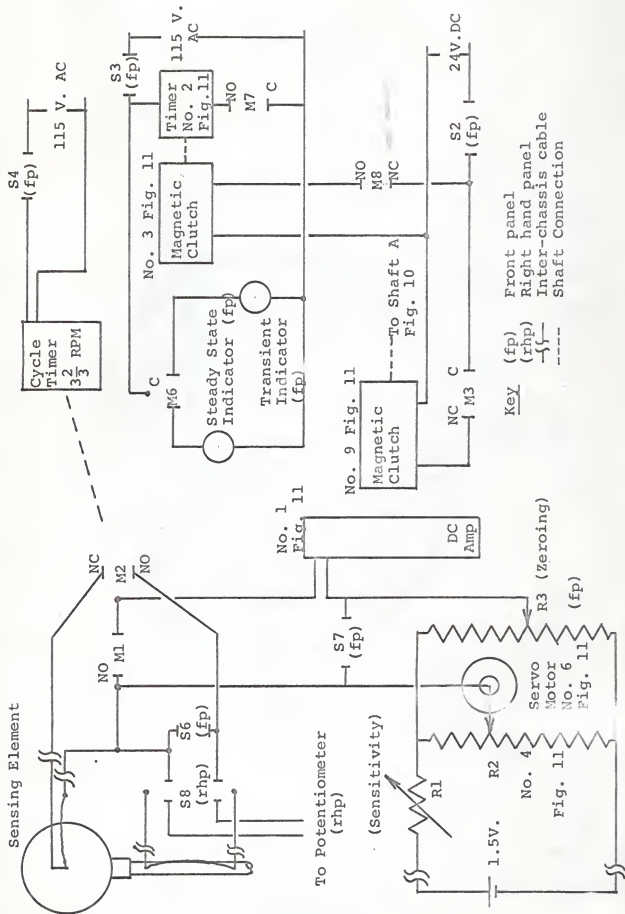


Figure 12. The Controller Schematic

Two cases are examined. The first is graphically portrayed in Fig. 13a. This shows sphere temperature response to a condition of about 120 MRT with an ambient air temperature of 80F.

Figure 13b shows the performance at several sensitivity settings for an MRT of 79F with an ambient air temperature of 76.6F. In each case the MRT is simulated by supplying electrical energy to the sphere surface with a fine constantan wire winding.

It is evident that for each case the 3/4 turn setting results in the most optimum controller operation.

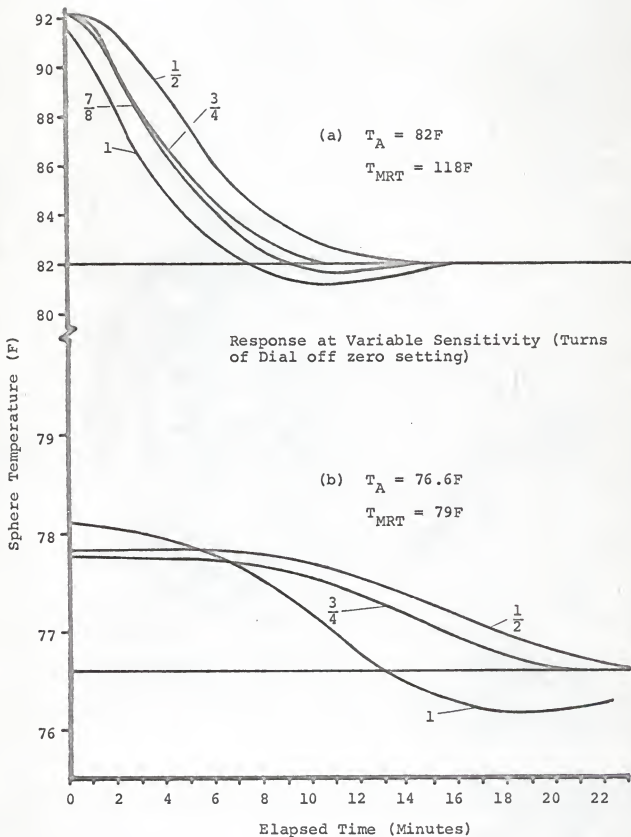


Figure 13. Controller Performance at Different Sensitivity Settings

## CHAPTER VI

### RESULTS

Figure 14 is a photograph of the complete radiometer systems. Other equipment required for MRT measurements includes a precision potentiometer and an accurate dry-bulb thermometer. The latter is shielded from radiation effects.

The radiometer was tested under a wide range of conditions in the test chamber at the Institute for Environmental Research at Kansas State University. The tests were composed of the following: 1) measurement of MRT both above and below air temperature, 2) measuring the effect of increasing the air velocity over the sensing element, 3) observing the dynamic response of the instrument to a changing room condition, and 4) measuring the effects of room lights on the measured MRT. Readings taken by the instrument are compared with those taken concurrently by the Minneapolis Honeywell two-sphere radiometer. No more than two persons were present for a given test. Table 1 gives the test results in chronological order.

For Test No. 1, room air temperature was set at 70F. The temperature of the walls, floor, and ceiling was controlled at 80F. The room lights were on. Both radiometers indicated an MRT of 80.5F for several consecutive readings.

Room air velocity effects were evaluated (Test No. 2) using a small blower and a hotwire anemometer. An increase of air

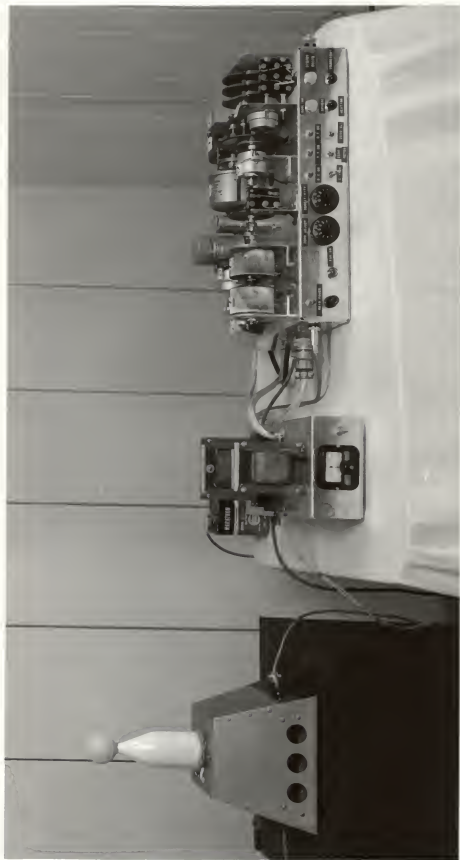


Figure 14. Photograph of Complete Radiometer Systems

TABLE 1

## RESULTS OF TEST CHAMBER MRT MEASUREMENTS

Test No.	Time	Air Temp. F	Chamber Surface Temp. F	Air Velo. fpm	R.H. %	Room Lights	Two-sphere Radiometer MRT F	Thermoelectric Radiometer MRT F
1	9:30AM	70	80	15-25	55	on	80.5	80.5
2	9:50AM	70	80	90	55	on	80.5	80.7
3	10:30AM	70	79.5	15-25	55	off for five minutes	79.6	79.5
4	11:30AM	70	80	15-25	55	off for one hour	79.7	80.2
5	2:00PM	70	74	15-25	55	on	77.0	75.8
6	4:00PM	84	76	15-25	30	on	79.7	79.0
7	9:30PM	84	98.5 to 99.5	15-25	30	off	-----	99.0

velocity, from the normal room velocity of 15-25 fpm, to 90 fpm changed the reading of MRT from 80.5F to 80.7F. This is an acceptable error to this author. It demonstrates that the instrument is essentially free from air velocity effects.

Evaluation of the effects of room lighting were made by measuring the MRT for the five minute period immediately after turning off the lights (Test No. 3) and also for a period after one hour of darkness (Test No. 4). The radiometer read an MRT of 79.5F at the end of the five minute period. The two-sphere radiometer read an average MRT of 79.6F for the five minute period. During this period the chamber surface temperatures dropped 1/2F. After one hour the surface temperatures were adjusted back to 80F. At that time the radiometer reading was 80.2F compared to a two-sphere radiometer reading of 79.7F

Test No. 5 is similar to Test No. 1 except that the difference in air and surface temperatures is reduced. The difference in readings by the thermoelectric radiometer and the two-sphere radiometer may be explained by the fact that the two-sphere radiometer does not reflect so large a portion of the visible spectrum as does the thermoelectric radiometer. (Ref. Fig. 7)

In Test No. 6 the air temperature was raised above the surface temperature. For these readings the controller cycled to the "sphere heating" mode. Readings were taken with 84F air temperature, 76F surface temperatures, and with lights on. The radiometer indicated an MRT of 79.0F as compared with a two-sphere radiometer reading of 79.7F.

For Test No. 7, the chamber surface temperature was raised to 100F. The lights were turned off. The indicated air temperature was 84F. The radiometer read an MRT of 99.0F. Because of the large gradient between surface temperature and air temperature the true chamber surface temperatures may have been close to 99.0F. The 100F surface temperature readings were made with thermocouples behind the wall surfaces. Spot checking of surface temperature with a digital thermistor thermometer resulted in readings of from 98.5F to 99.5F. The two-sphere radiometer was not used for this test.

The dynamic response of the instrument (Ref. Fig. 13) was checked during the changeover of chamber conditions. Chamber surface temperatures may be changed rapidly. Changes in air temperature require more time. It was discovered that the instrument could follow air temperature changes but that it lagged behind changes in surface temperatures. It is believed, however, that the response time of the instrument is adequate for environmental studies.

It is concluded that subject to previously stated conditions (Ref. Chapter III, Page 11), the present radiometer provides a convenient and accurate method of measuring the MRT of rooms. The complete system has been operated for more than 100 hours with no difficulty. Readings taken in the previously discussed tests indicate that the instrument has an accuracy within the limits of accuracy estimated in Appendix A.

The continuation of the development of the present radiometer will include several phases. The effects of changes in relative humidity are to be analysed. An instruction manual is to be prepared for future reference. The radiometer will be used for human comfort studies in conjunction with the Minneapolis Honeywell two-sphere radiometer.

## LIST OF REFERENCES

1. Aagard, R. L. "Convection-Free Instrument for Measuring Infrared Radiation in the Atmosphere." Rev. of Sci. Instruments, November 1958, 29: 1011-1016.
2. ASHRAE Standard 55-66, Thermal Comfort Conditions, Copyright 1966, New York.
3. Bell, J. H., Jr. Cryogenic Engineering. Englewood Cliffs, N.J.: Prentice Hall, Inc., 1963.
4. Benzinger, T. and C. Kitzinger. "A 4 $\pi$ -Radiometer." Rev. of Sci. Instruments. July 1950, 21: 599-604.
5. Brown, A. I., and S. M. Marco. Introduction to Heat Transfer. New York: McGraw-Hill Company., 1958.
6. Dahl, A. I. Temperature-Its Measurement and Control in Science and Industry. New York: Reinhold, 1962.
7. Funk, J. P. "Improved Polythene-Shielded Net Radiometer." J. Sci. Instruments., June 1959, 36: 267-270.
8. Gagge, A. P., G. M. Rapp and J. D. Hardy. "The Effective Radiant Field and Operative Temperature Necessary for Comfort with Radiant Heating." Presented at the Winter Meetings of ASHRAE. Detroit, Michigan. January, 1967.
9. Gibson, John E., Non Linear Automatic Controls. New York: McGraw Hill Co., 1963.
10. Goldsmith, A., T. E. Waterman and H. Hirschhorn. Handbook of Thermophysical Properties of Solid Materials, New York: The McMillan Co., 1961.
11. Hager, N. E., Jr. "Absolute Differential Radiometer." Rev. of Sci. Instruments. September 1963, 34: 1028-1034.
12. Houghton, B. A. and A. W. Brewer. "A New Radiometer." J. Sci. Instruments., May 1954, 31: 184-187.
13. Loser, J. B., and others. Thermophysical Properties of Thermal Insulating Materials, Technical Documentary Report No. MC-TDR-64-5. February 1964, Midwest Research Institute, Kansas City, Missouri.

14. Moran, J. P. "Radiant Energy Measurement." Instr. and Contr Syst., July 1965, 38: 127-128.
15. Richards, C. H., A. M. Stoll, and J. D. Hardy. "The Panradiometer," Rev. of Sci. Instruments, December 1951, 22: 925-34.
16. Stoll, A. M. "A Wide Range Thermistor Radiometer." Rev. of Sci. Instruments, February 1954, 25: 184-187.
17. Sutton, D. J. and P. E. McNall, Jr., Two-Sphere Radiometer. Minneapolis Honeywell Research Report GR2462-R2. Minneapolis, Minnesota. 1953.
18. Treharne, R. W. and H. W. Trolander. "Wavelength-Independent, Direct-Reading Radiometer." J. Sci. Instruments., 1965, 42: 699-701.
19. Tunmore, B. G. "A Simple Radiometer for the Measurement of Radioactive Heat Exchange Between Buildings and the Environment." J. Sci. Instruments., 1962, 39: 219-221.

## APPENDIX A

### Theoretical Error Analysis

Errors in the instrument arise as a result of heat transfer effects and from errors in the measurement of physical parameters. The errors which are the result of heat transfer are first to be presented.

#### Errors Resulting From Heat Transfer Effects

##### 1. Sensing Element Temperature Gradients

An input of 5 Btu/Hr. is assumed. This corresponds to an MRT of 130F with 70F ambient air. The sphere is divided into 20 slices. As shown in Fig. 15 each subtends an angle of  $9^\circ$ . Radiation is assumed to fall equally on each unit area of the spherical surface. The outer surface of each slice has a different surface area, and a corresponding different heat input. All incoming radiation is assumed to be conducted successively from slice to slice through the sensing element skin. The temperature change across each slice depends on the effective cross sectional area of the slice, the thermal conductivity of the silver, the length of the path, and the amount of heat flow. The conductivity is taken as 242 Btu/Hr F ft (10). The other parameters are variable. Table 2 is a summary of the calculations.

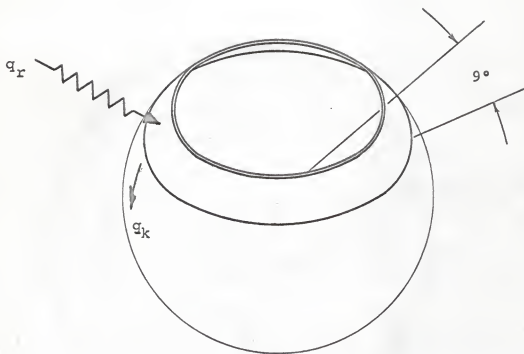


Figure 15. Model for Sphere Temperature Gradient Calculations

TABLE 2

## TEMPERATURE GRADIENT CALCULATIONS FOR THE SENSING ELEMENT

No.	Radiation Input Btu/Hr	Average Conduction in slice Btu/Hr	Average Cross-section of Slice Ft <sup>2</sup>	Length of Conduction Path "L" Ft	Temperature drop across slice F	Surface Temperature Profile F
1	0.034	0.017	0.0007	0.013	0.0013	70
2	0.088	0.075	0.00210	0.013	0.0019	69.9981
3	0.150	0.197	0.00330	0.013	0.0032	69.9949
4	0.205	0.379	0.00456	0.013	0.0045	69.9904
5	0.255	0.604	0.00566	0.013	0.0056	69.9848
6	0.298	0.882	0.00663	0.013	0.0072	69.9776
7	0.335	1.200	0.00745	0.013	0.0087	69.9689
8	0.362	1.545	0.00805	0.013	0.0130	69.9559
9	0.383	1.920	0.00848	0.013	0.0123	69.9436
10	0.390	2.300	0.00862	0.013	0.0145	69.9291
11	0.390	2.690	0.00862	0.013	0.0169	69.9122
12	0.383	3.081	0.00848	0.013	0.0198	69.8924
13	0.362	3.450	0.00805	0.013	0.0232	69.8692
14	0.335	3.800	0.00745	0.013	0.0276	69.8416
15	0.298	4.117	0.00663	0.013	0.0337	69.8079
16	0.255	4.385	0.00566	0.013	0.0413	69.7666
17	0.205	4.625	0.00456	0.013	0.0550	69.7116
18	0.150	4.800	0.00330	0.013	0.0790	69.6326
19	0.088	4.920	0.00210	0.013	0.1270	69.5056
20	0.034	5.000	0.000700	0.013	0.1800	69.3256
Total	5.000					

The second to last column gives the temperature change across a given slice. The total gradient for slices 1 through 19 is found to be 0.4944F. It is noticed that the first 16 slices have a total temperature drop of less than 0.25F. Thus the major portion of the surface is very nearly an isothermal surface. If the entire surface were 0.25F from the ambient air temperature an error due to convection heat transfer of  $0.0501 (0.25)^{1.25}$  Btu/Hr. would result (ref. Appendix D). This amounts to 0.0087 Btu/Hr. or an error in MRT of 0.1F. The percentage error is  $\frac{(0.0087)(100)}{5}$  or 0.17%.

## 2. Heat Meter Insulation Error Calculation

An input of 5 Btu/Hr is assumed. This heat must be conducted down the heat meter. Ideally no heat should flow through the heat meter insulation, for this would mean that the amount of energy flowing down the heat meter would not change. Any change in this amount of energy will result in an error.

Figure 16 shows the model used for calculation of errors due to radial heat flow in the insulation. The glass shell is assumed to be absent. Thus only the insulating material is given credit for reducing heat flow. The tapered portion of the insulator is divided into four parts. The lower parallel walled portion is taken in one part.

Table 3 is a summary of the calculations. The summation of the last column is left as a function of K, the apparent thermal conductivity of the insulation material. At  $10^{-3}$  Torr the value

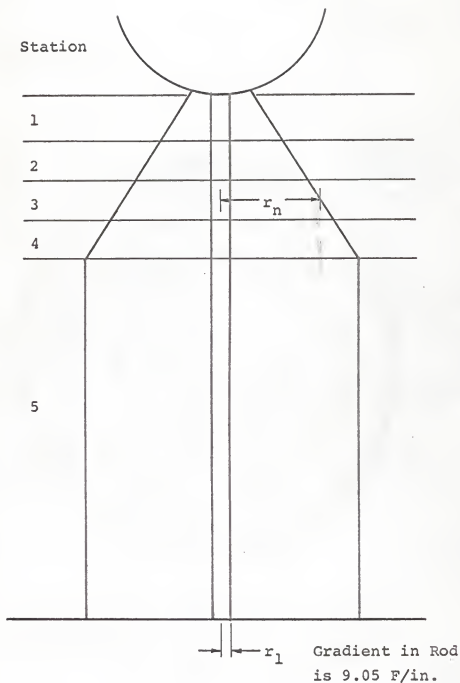


Figure 16. Model for Heat Meter Error Calculations

TABLE 3

## RADIAL HEAT TRANSFER CALCULATIONS FOR THE HEAT METER INSULATION

Station	Mean $\Delta T$	$2\pi L\Delta T$	$\frac{r_2}{r_1}$	$\frac{r_2}{\ln \frac{r_2}{r_1}}$	$\frac{2\pi L\Delta T}{\ln \frac{r_2}{r_1}}$ (Ft F)	Q (Btu/Hr)
1	2.4	.785	4.27	1.45	.54	0.54K
2	8.2	2.684	6.94	1.94	1.38	1.38K
3	14.0	4.656	9.60	2.26	2.06	2.06K
4	19.8	6.386	11.70	2.46	2.59	2.59K
5	36.4	57.450	12.30	2.51	22.80	22.80K
Total						29.37K

of K for Santocel A is 0.001 Btu/Hr F ft (13). This means that the total radial heat flow is on the order of 0.030 Btu/Hr for an axial heat flow of 5 Btu/Hr. This results in an error in the reading of MRT of about 0.5F. The error may also be expressed as a percentage of the difference of the ambient air temperature and the MRT. This percentage is  $\frac{0.03}{5.00} \times 100$  or 0.6%. Thus in reading an MRT of 75 F in ambient air at 70F, an error of (0.006)(5) or 0.03F results.

### 3. Thermocouple Leadwire Conduction Error Calculation

The iron-constantan thermocouple lead wires conduct a small amount of heat in a path parallel to the silver heat meter rod. For 5 Btu/Hr of energy flowing in the heat meter, the energy shunted through the leadwires may be found by the following considerations. Both parallel paths have the same temperature gradient. The ratio of the areas of the 10 lead wires (0.010" dia.) to the area of the silver rod (0.1867" dia) is .0287. The ratio of the average thermal conductivity of the iron (45 Btu/Hr Ft. F) and constantan (13.1 Btu/Hr Ft F) to the thermal conductivity of silver (242 Btu/Hr Ft F) is 0.12. Therefore the heat flow shunted through the leadwires is (5)(.0287)(.12) or 0.0172 Btu/Hr. This amounts to an error of  $\frac{(.0172)100}{5.000}$  or 0.34% of a given MRT reading.

### 4. Axial Temperature Gradients in the Glass Shell

The bottom of the glass shell which surrounds the insulation is connected to the thermoelectric module and will be subjected to axial temperature gradients. Therefore, heat is transferred from

the sensing element into the glass shell. It is assumed that the temperature gradient in the glass shell is equal to the heat meter gradient at 5 Btu/Hr or 9.05F/in. The minimum cross-sectional area of the glass is  $0.00131 \text{ ft}^2$ . The thermal conductivity of the glass is 0.33 Btu/Hr F ft. From these data the maximum amount of heat shunted down the glass shell is 0.0467 Btu/Hr. This results in a percentage error of  $\frac{(0.0467)(100)}{5.0}$  or 0.93%.

#### Errors in Measurement of Physical Parameters

The errors to be treated in this section arise from the fact that perfect measurements of physical parameters are not possible. The accuracy of the instrument is directly dependent upon the accuracy of measurements made by this author and also upon the accuracy of data used. The physical parameters in the order discussed are length, temperature, emissivity, thermal conductivity, and thermoelectric potential.

The errors in measuring the distance between thermocouples and the diameter of the heat meter rod are considered. For the former, accuracy is within  $\pm 0.01$  in. Thus for the 3.87 in distance an error of  $\frac{(0.02)(100)}{3.87}$  or 0.516% is possible. The diameter of the heat meter rod was measured to within  $\pm 0.00015$  in. This means that an error in cross-sectional area of  $\frac{(0.0003)^2(100)}{(0.1867)^2}$  or 0.00026% is possible.

The inability of the heat meter thermocouples to measure the actual temperature of the rod at the point they are attached can result in an error. An attempt at calculating this error is not

made. The thermocouples are, however, in good thermal contact with the rod so that this error should be small.

The emissivity of the sensing element coating was taken as 0.87. This number is believed to be within 1.0% accuracy.

The thermal conductivity of the silver rod used was taken from a recent source (10), which is thought to be the most accurate data available. Therefore, no estimate of an error in thermal conductivity is made.

The errors resulting from the thermoelectric properties of the thermocouple circuits have previously been discussed (ref. Appendix C). As noted in Appendix C, errors of this type are negligible for the majority of MRT measurements.

The sum of all errors considered is less than 5%. Errors due to the inability of the control mechanism to control the sensing element at precisely the ambient air temperature are also significant. (Ref. Chapter VI.) From an error standpoint the physical design of the radiometer proper is considered acceptable.

## APPENDIX B

The hollow silver sphere used for the sensing element was made by a method which deserves being permanently recorded.

The method consists of a cold-work process combined with an annealing process. A short length of steel pipe of a diameter twice that of the sphere being formed is filled with molten lead. The level of the lead is slightly higher than the edge of the pipe. A silver disc of diameter 50% greater than the sphere being made is cut out and centered on the lead surface. A steel ball of diameter equal to the sphere is centered on the silver disc and hand-held. A large ball peen hammer is used to strike the ball into the lead. As the hemisphere is formed, wrinkles will form on the edges of the disc. The silver is annealed by heating to 800F and quenching in water. This softens the silver so that wrinkles may be removed with light tapping.

After several successive cycles of cold working and annealing the silver is gathered around the ball to the equator. It is then removed and the leading edge is lightly honed to produce a hemisphere. The process is repeated and the two hemispheres are silver-soldered together.

It is advisable to experiment with copper sheet until proficiency is attained. The copper has similar properties and is considerably less costly and easier to procure.

## APPENDIX C

### The Heat Meter Design

The heat meter is designed such that the millivolt output of the heat meter thermocouples is numerically equal to the heat transfer in the metering rod in Btu/Hr. This provides for convenient use of the instrument.

On page 56, Dahl gives improved values for iron-constantan thermocouples (6). Between 60F and 70F the output of an iron-constantan thermocouple is 0.02856 millivolts/F. At a rate of 5 Btu/Hr transferred down the 0.1867 in diameter metering rod the temperature gradient is 9.05 F/in. This results in an output of 0.2583 millivolts/thermocouple/in. Since a 5 millivolt signal is required, the product of the number of thermocouples times the spacing between each is  $\frac{5.0}{0.2583}$  or 19.36. The maximum available distance along the metering rod is 4 inches. Thus 5 thermocouples are used at a spacing of  $\frac{19.36}{5.0}$  or 3.87 inches.

An error results from the very slight non-linearity of the thermocouple response curves. For readings of MRT between 50F and 90F in ambient air at 70F this error is negligible. Within the maximum range of the instrument this error is limited to 1.3%.

#### Calculation of the Constant Term in [5], Chapter IV

An emissivity at the long wave-lengths of 0.87 (ref. Fig. 7) is used. On page 65 of their text Brown and Marco express the

constant  $\sigma$  as  $0.173 \times 10^{-8}$  Btu/Hr Ft<sup>2</sup> F<sup>4</sup>. The effective area of the 1.95" diameter sphere is equal to the total surface area minus the part covered by the heat meter insulation or 0.079881 ft<sup>2</sup>. The product of these terms is 0.012023.

## APPENDIX D

### Error Signal Generation

The basic equation for the analysis of error signal generation is repeated for convenience.

$$0.012023 \left[ \left( \frac{T_{MRT}}{100} \right)^4 - \left( \frac{T_E}{100} \right)^4 \right] = 0.0501 (T_E - T_A)^{1.25} + 0.104 (T_E - T_A) \quad [1]$$

The constant on the left side of [1] is developed in Appendix C. The first term on the right side accounts for convection heat exchange and may be found as follows.

$$q_c = h_c A (T_E - T_A) \quad [2]$$

where

$q_c$  = convection loss (Btu/Hr)

$h_c$  = convection film coefficient (Btu/Hr ft<sup>2</sup>F)

$A$  = Effective spherical surface area (ft<sup>2</sup>)

$T_E$  = sphere surface temperature (F)

$T_A$  = air temperature (F)

On pages 165-168 Brown and Marco provide a method for calculating  $h_c$  (5).

$$h_c = C \frac{K}{L} [a L^3 (T_E - T_A)]^d \quad [3]$$

where

C = constant equal to 0.63 for spheres in this temperature and size range, (dimensionless)

K = thermal conductivity of air at the average film temperature ( $0.014 \frac{\text{Btu}}{\text{Hr-ft}^2\text{-F}}$ )

L = sphere radius (.0812 ft.)

a = Modulus,  $1.5 \times 10^6$ , (dimensionless)

d = empirically determined exponent, 0.25 for spheres in this temperature and size range.

[3] reduces to

$$h_c = 0.6274(T_E - T_A)^{.25} \quad [4]$$

so that [2] becomes

$$q_c = 0.0501(T_E - T_A)^{1.25} \quad [5]$$

The conduction heat transfer resulting from the difference  $(T_E - T_A)$  is equal to  $0.104(T_E - T_A)$  by means of calculations identical to those in the portion of Appendix C dealing with the heat meter design.

Table 4 shows the calculation of  $T_{MRT}$  from [1]. These results are plotted in Fig. 8.

TABLE 4

## ERROR SIGNAL CALCULATIONS

Ambient Air Temperature F	Sphere Temperature F	$T_E - T_A$ F	$\frac{9}{C} \frac{BTU}{hr}$	$\frac{9}{k} \frac{BTU}{hr}$	$\frac{9}{C} \frac{BTU}{hr}$	$\frac{9}{C} \frac{BTU}{hr}$	$T_{MRT}$ F
70	71	1	0.0501	0.104	0.1541	0.1541	72.2
70	72	2	0.1191	0.208	0.3271	0.3271	74.5
70	73	3	0.1970	0.312	0.5090	0.5090	77.0
70	74	4	0.2830	0.416	0.6990	0.6990	79.5
70	75	5	0.3750	0.520	0.8950	0.8950	82.1
70	76	6	0.4710	0.624	1.0950	1.0950	84.6
70	77	7	0.572	0.728	1.3000	1.3000	87.3
70	78	8	0.672	0.832	1.5040	1.5040	89.9
70	79	9	0.782	0.936	1.7180	1.7180	92.5
70	80	10	0.829	1.040	1.9320	1.9320	95.1

#### ACKNOWLEDGEMENTS

The author is highly indebted to Dr. Preston E. McNall, Jr. for his excellent guidance and encouragement during all phases of the project.

Gratitude is also extended to Dr. Ralph G. Nevins for arranging for the financial support; to Dr. James M. Bowyer, Jr. for his technical direction in several difficult problem areas; to Mr. John C. Black for assisting in the development of the control mechanism; and to Mr. Donald R. Frikken and Mr. Thomas Darnell for aid in preparation of the illustrations.

VITA

David L. Braun

Candidate for the Degree of

Master of Science

Thesis: AN OMNIDIRECTIONAL CONVECTION NULLING THERMOELECTRIC  
RADIOMETER FOR ENVIRONMENTAL APPLICATIONS

Major Field: Mechanical Engineering

Biographical:

Personal Data: Born at Webster, South Dakota, February 19,  
1939, the son of Louis F. and Myrene C. Braun.

Education: Attended grade school in Rapid City, South  
Dakota; graduated from Rapid City High School in 1957;  
received the Bachelor of Science degree in Mechanical  
Engineering from South Dakota School of Mines in June,  
1961; candidate for Master of Science degree, May, 1967.

Professional experience: A total of 30 months of diversified  
experience in the oil business; served 24 months in the  
United States Army Ordnance Corps.

AN OMNIDIRECTIONAL CONVECTION NULLING THERMOELECTRIC  
RADIOMETER FOR ENVIRONMENTAL APPLICATIONS

by

DAVID LLOYD BRAUN

B. S., South Dakota School of Mines, 1961

---

AN ABSTRACT OF A MASTER'S THESIS

submitted in partial fulfillment of the

requirements for the degree

MASTER OF SCIENCE

Department of Mechanical Engineering

KANSAS STATE UNIVERSITY  
Manhattan, Kansas

1967

Name: David Lloyd Braun Date of Degree: June 4, 1967

Institution: Kansas State University

Location: Manhattan, Kansas

Title of Study: AN OMNIDIRECTIONAL CONVECTION NULLING THERMO-ELECTRIC RADIOMETER FOR ENVIRONMENTAL APPLICATIONS

Pages in Study: 63 Candidate for Degree of Master of Science

Major Field: Mechanical Engineering

Scope and Method of Study: The thesis describes the design and development of a thermoelectric radiometer and associated control equipment. The radiometer sensing element is composed of a two inch hollow silver sphere coated with a material approximating the spectral emissivity characteristics of human skin. This sphere is connected mechanically and thermally to a thermoelectric module by means of an insulated silver heat metering rod.

The magnitude and polarity of the DC thermoelectric module signal is controlled such that the sensing element temperature equals the ambient air temperature. In this way, convection effects are nulled. The conduction heat transfer up or down the heat metering rod is equal to the net radiation emitted or received by the sensing element. This net radiation is used to calculate the effective Mean Radiant Temperature (MRT) of the environment in which the instrument is operating.

Control is accomplished by periodic adjustment of an autotransformer by means of a continuous balance servo-mechanism. The signal for the latter is the output of a

differential thermopile measuring the difference in temperature of the sensing element and the ambient air. The magnitude and polarity of the DC thermoelectric module signal depends on the angular position of the autotransformer shaft. Continuous adjustments of the module current are made in order to retain the sphere-air thermopile signal at or near the zero value.

The controller includes a detector which automatically indicates when the radiometer systems have reached steady-state conditions. Readings of the heat metering rod are made only during steady-state conditions.

Findings and Conclusions: The radiometer was used to measure the MRT of the test chamber at the Institute for Environmental Research at Kansas State University. Readings are compared with those taken by the Minneapolis Honeywell two-sphere radiometer and with indicated chamber surface temperatures. For a darkened room with chamber surface temperatures ranging from 98.5 F to 99.5 F the radiometer indicated an MRT of 99.0 F. For the majority of readings with lights on, the present radiometer indicated an MRT lower than that measured by the Minneapolis Honeywell two-sphere radiometer. The latter instrument indicates values of MRT higher than those that would be made by human subjects.

It is concluded that the thermoelectric radiometer provides a convenient and accurate method for evaluating the MRT of rooms.

MAJOR PROFESSOR'S APPROVAL

P. E. M. G. Hall